DIRECT TENSION TESTING OF SFRC – SOME PECULIAR EFFECTS OF THE END RESTRAINTS

ALI AMIN[*], TOMISLAV MARKIĆ[†], AND WALTER KAUFMANN[†]

[*] The University of Sydney
Sydney, Australia
e-mail: ali.amin@sydney.edu.au

[†] ETH Zürich
Zürich, Switzerland
e-mail: {markic, kaufmann}@ibk.baug.ethz.ch

Key words: Steel Fiber Reinforced Concrete, Uniaxial Tension Test, Boundary Conditions.

Abstract: In principle, a direct tension test is the ideal test that should be used in experimentally determining the softening, or residual, parameters of steel fibre reinforced concrete (SFRC). In the context of design, these material properties are then used to feed into models for shear, flexure etc. This is the approach that has been adopted in the recently released standard for the design of concrete structures in Australia (AS3600-2018). However, there are many parameters which may influence the results of the uniaxial tension test, and the choice of boundary conditions for the test is one of the most relevant ones. Three boundary or end conditions are possible: fixed-fixed, fixed-rotating, and rotating-rotating. In this paper, results of uniaxial tensile tests on twelve identical SFRC direct tension specimens tested with the end conditions listed above are presented. Each condition exhibits behaviours not present in the theoretically ideal tensile softening curve and investigating this is the focus of the present study. It is concluded that the fixed-rotating end conditions serves as a compromise to the issues associated with the other test setups and seems to be more suited for uniaxial tension testing of softening SFRC.

1 INTRODUCTION

The primary objective of adding fibres (steel, polypropylene or otherwise) to concrete is to bridge cracks once they form. This fibre-bridging action provides some post cracking resistance to the concrete when stressed in tension. Quantifying this post-cracking behaviour defines the material for design. In principle, a direct tension test is the ideal test that should be used to determine the softening, or residual, parameters of steel fibre reinforced concrete (SFRC) [1-3]. Unlike results from tests of prism in bending or round panel tests, the results from the uniaxial tension test (UTT) do not require an inverse analysis, or other methods to post-process. That is, the results from the uniaxial tension test can be directly put into design models (i.e. for shear, flexure etc.). Another advantage of uniaxial tensile loading conditions is that Mode I failure takes place; this is considered the most relevant failure mode of quasi-brittle materials such as concrete.

Despite their apparent simplicity, several difficulties emerge when conducting direct uniaxial tension tests on SFRC. The first is the nature of the test setup. Along with specimen size, specimen shape, heterogeneity of the material, and presence of notches, the boundary conditions at the specimen ends are one of the parameters that most heavily influence the results of a uniaxial tension test. The type of boundary conditions that should be applied to a uniaxial tension test continues to be an ongoing matter of discussion in the

scientific community [4, 5] and is the motivation for this research.

The categories of boundary conditions are essentially limited to rotating ($\theta \neq 0$) and/or fixed (non-rotating) ($\theta = 0$) boundary conditions. Rotating boundaries allow the specimen ends to freely rotate (around all three axes) during the test; fixed boundaries restrain rotation of the specimen ends by the bending stiffness of the test setup. An ideal boundary condition would apply uniform uniaxial tension to the specimen, and produce a stable tensile softening curve. Hence, fixed ends providing homogeneous load introduction (uniform displacements) at the specimen ends would basically be advantageous. However, in laboratory experiments, the heterogeneity of the material, the specimen manufacturing, and the gripping and alignment of the specimen in the loading frame are not easily controlled and may result in secondary bending moments being induced to the specimen.

Under rotating boundaries, the crack will initiate and propagate from its weakest location and traverse the section. Under fixed boundaries, this will also happen, but as the specimen boundaries are forced to remain parallel during crack propagation, an eccentricity of the applied load induces a bending moment into the sample. Due to this bending moment, the crack will be prevented from propagating further through the section until the other side of the specimen begins to fracture. This can result in two unique cracks developing within the specimen [6].

The test method proposed in the recently released standards AS5100.5 (2017) [7] and AS3600 (2018) [8] have countered this by adopting one fixed and one rotating boundary in their testing arrangement of SFRC in uniaxial tension. By including a universal joint at one end of the specimen, the intention is that accidental residual tensions that may develop as a result of gripping the specimen can be minimised. The testing arrangement adopted by the Australian codes is illustrated in Figure 1.

This paper presents results of testing conducted on twelve identical SFRC specimens shaped according to [7, 8] in uniaxial tension with the three boundary configurations listed above. The aim is to provide data on the effects of the different boundary conditions on the tensile softening behaviour of SFRC, with the eventual goal to determining which boundary system is best suited for use in a standardised test.

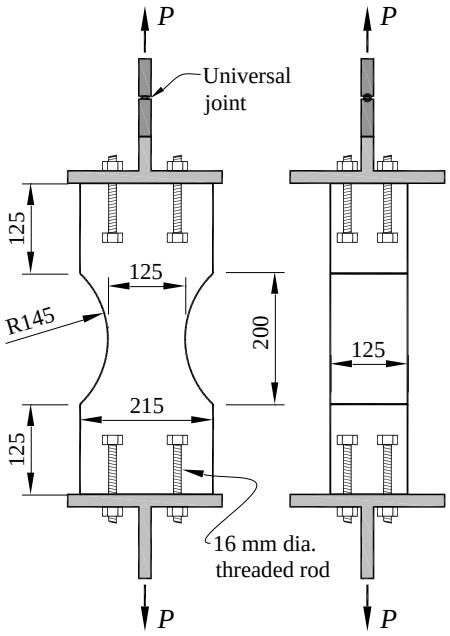

Figure 1: Details of UTT for SFRC

2 UNIAXIAL TENSION TEST FOR SFRC

The arrangement of the uniaxial tension test of [7, 8] was adapted from [9] and was selected based on its ease of casting and the reduction of stress concentrations that can predetermine a crack path.

The evolution of the development of the uniaxial tension specimen or "dogbone" specimen proposed by van Vliet [9] is illustrated in Figure 2. van Vliet first reasoned that the preferred specimen for uniaxial tension testing would be one with sporadic boundaries (Figure 2a). However, a setup of this nature does not lend itself to practical considerations and the specimen should be given finite dimensions, which are characterised by a ratio between the height, width and thickness of the specimen (Figure 2b). An enlarged end followed by a prismatic cross section (Figures 2c and 2d) has recently gained popularity particularly from the University of Toronto [10-12]. This shape

allows for the crack to initiate and propagate at the weakest spot in the tapered section of the specimen, whilst also overcoming a number of issues associated with connecting the specimen to the testing frame. However, the main issue with this shape is the strong variation in the tensile stress distributions, particularly at the rounded corners. Take for instance, the linear elastic principal tensile stress distributions shown in Figures 3a and 3b for dogbone specimens presented in Figures 2d and 2e, respectively. For tensile tests, the specimen of Figure 3b is more suited because only a marginal stress gradient develops, whereas the stress concentrations in the corners of Figure 3a tend to force crack nucleation in those areas. This can be seen from the photographs of uniaxial tension test specimens reported in Luo [11] and shown in Figure 4.

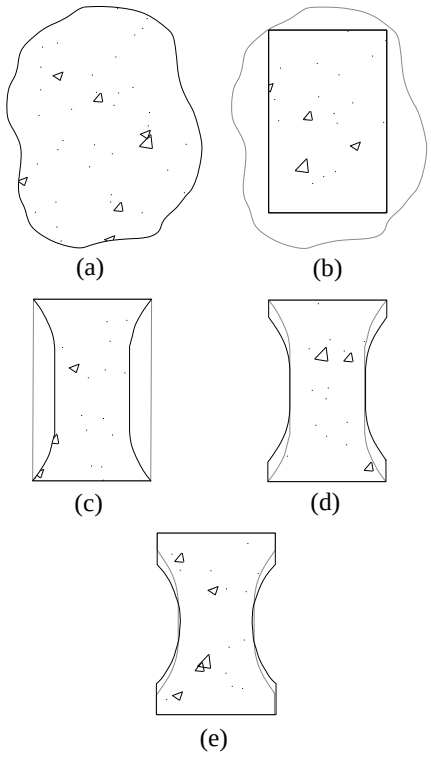

Figure 2: Evolution of van Vliet [9] UTT geometry

The sample geometry [7, 8] (shown in Figure 1), being approximately 40% narrower in the midsection than at its ends, permits for failure to occur within a reasonably well defined region. Furthermore, no notches are required and therefore the dominant crack does not pass through a pre-determined plane. The use of notches, from a fracture mechanics viewpoint results in strong deviations from a 'pure' uniaxial state of stress in a specimen. For more information, the reader is referred to [1]. The specimen thickness of 125 mm minimizes the wall effect on fibre distribution, allows for ease in handling and may be considered as representative of a continuum on a large scale.

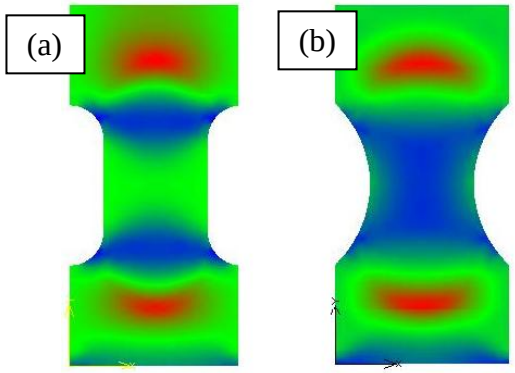

Figure 3: Linear elastic principal tensile stress distribution of two different UTT specimens

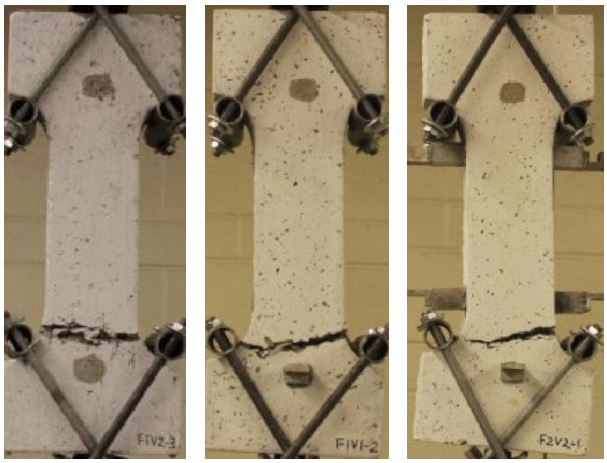

Figure 4: Photographs of [11] failed UTT specimens.

Another difficulty associated with the uniaxial tension test worth highlighting is the method of attachment of the specimen to the testing machine in a way that minimizes any influence on the results. Three methods have been adopted by researchers and each have their advantages and disadvantages. Mechanical grips can be used to apply tensile load to the specimen, however the act of gripping the specimen causes a biaxial state of stress near the grips [1]. The biaxial tensile-compression strength of concrete is weaker

than its uniaxial tensile strength, so if a prismatic or cylindrical specimen is used, it will tend to fail near the grips. The second method is to glue the specimen to the steel plates of the testing device, typically with a commercial two-part epoxy resin. This may require some trial and error to determine if the epoxy is sufficiently strong to achieve a satisfactory bond. This method is also costly in time and labour. The third method is to embed threaded rods partially within the specimen during casting (see Figure 1). When the specimen is ready for testing, it can then be bolted to the end platens of the testing device. However, the presence of the threaded rods within the specimen can generate localised stress concentrations, which may distort the results of unnotched prismatic or cylindrical specimens and cause them to fail close to the boundary attachment point. For the dogbone specimens adopted by the Australian Codes, the tip of the threaded rods is sufficiently far from the point at which the width of the specimens begin to decrease and hence the localised stress concentrations are far from the point of failure, and therefore unlikely to significantly affect the results.

3 EXPERIMENTAL PROGRAM

In this study, an experimental program was conducted to investigate the pre- and post-cracking behaviour of a single SFRC mix through uniaxial tension tests with varying boundary conditions (fixed-fixed (FF), rotating-rotating (RR) and fixed-rotating (FR)). Four specimens were manufactured for each test set up. The steel fibres were 35 mm long, had a diameter of 0.55 mm and an ultimate notional tensile strength of 1340 MPa. The fibre dosage used in this study was 60 kg/m^3. The concrete was supplied by a local ready mix plant and was delivered to the laboratory facility without the fibres included in the mix. The specified concrete compressive strength was 40 MPa (the measured cylinder concrete compressive strength at time of testing was 63 MPa) and the coarse aggregate used was basalt with a maximum particle size of 10 mm. The fibres were added to the agitator on site and mixed for ten minutes prior to casting the specimens. A standard slump test was used to assess that workability of the fresh SFRC and the measured slump was found to be 200 mm.

The specimens were cast horizontally in lubricated stainless steel moulds using a similar procedure as outlined in [13]. That is, the centre portion of the mould was filled to approximately 90% of the height of the specimen, which was then followed by pouring of the ends. The moulds were lightly externally compacted. To ensure uniform distribution of the fibres through the cross section of the sample the use of internal vibrators is not recommended as they tend to disperse the fibres and may leave behind regions of concrete without any fibres.

The dogbone specimens were tested in a 1MN Instron servo-hydraulic universal testing machine (UTM). To measure strain (and crack opening displacement), transducers (LVDT or LSCT) were fixed to each of the four sides of the specimen over a gauge length of 230 mm. The threaded rods protruding from the specimens were bolted to end plates and connected to the UTM. Photographs of the three test setups highlighting the different boundary conditions are presented in Figure 5. Load was applied to the specimen using ram displacement control, initially at a rate of 2.50 mm/h until the formation of the dominant crack. After cracking, the rate was increased to 8.00 mm/h until the measured crack opening displacement (COD) reached 2 mm, with additional increases in the rate introduced as the test progressed. It is noted that the UTM used in this study was unable to run the tests via strain control.

4 TEST RESULTS

In the analysis of the dogbone specimens, the following assumptions were made:

(i) the elastic deformations of the concrete near the vicinity of the crack are negligible relative to the opening of the crack;
(ii) shape induced tensile stress concentrations are small and can be

ignored; and

(iii) the uncracked concrete undergoes elastic unloading.

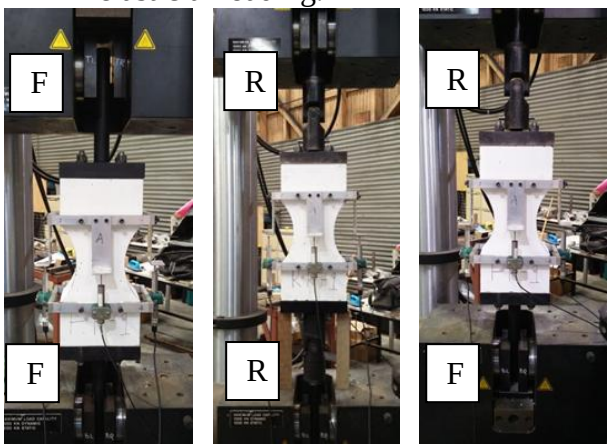

Figure 5: Photographs of UTT tests

The pre- and post-cracking experimental results compensated for the wall effect [14] for each test configuration are presented in Figure 6. In Figure 6, each curve represents the average value of the four readings obtained from the transducers for each test (this is elaborated below). Prior to cracking the response is expressed in terms of nominal stress (taken at the most narrow cross-section of the specimen) versus strain. After cracking, results are expressed as stress vs COD. Readings from each transducer are presented elsewhere [15].

In general the specimens (regardless of boundary condition) tended to behave similarly overall. The response prior to cracking was approximately linear. Close to peak stress, the response became softer due to micro-cracking and, after the peak load was reached, a sharp reduction in load and a significant opening of the dominant crack occurred. Significant elastic strain energy was stored in the testing frame and the specimen, and hence no displacement data is available between the matrix first cracking and the point where the cracking stabilized. This effect was less pronounced for the FF and FR series. The dogbones in the FF series exhibited a "bump" in the tensile softening region of the response up until a COD of ~1 mm. This bump is a relatively large variation from the freely rotating tests; [1] suggested that this bump is a consequence of non-uniform cracking of the heterogeneous material and the ability of the specimen to redistribute stresses in the experiment. In some instances in the FF series, two separate cracks initiated, however these cracks would soon join. The long tail of the curves reflects the progressively smooth residual capacity of the specimens. It is noteworthy that higher fracture energies (defined as the area under the stress-COD curves) were measured for series FF and FR than for series RR. A summary of the recorded material properties for each specimen (f_{ct}, E_t, f_{ct}, and $f_{0.5}$) are tabulated for reference in Table 1. It is interesting to note that the tensile strength of the FF specimens is consistently lower than the RR and FR series – this is thought to be a by-product of induced eccentricities.

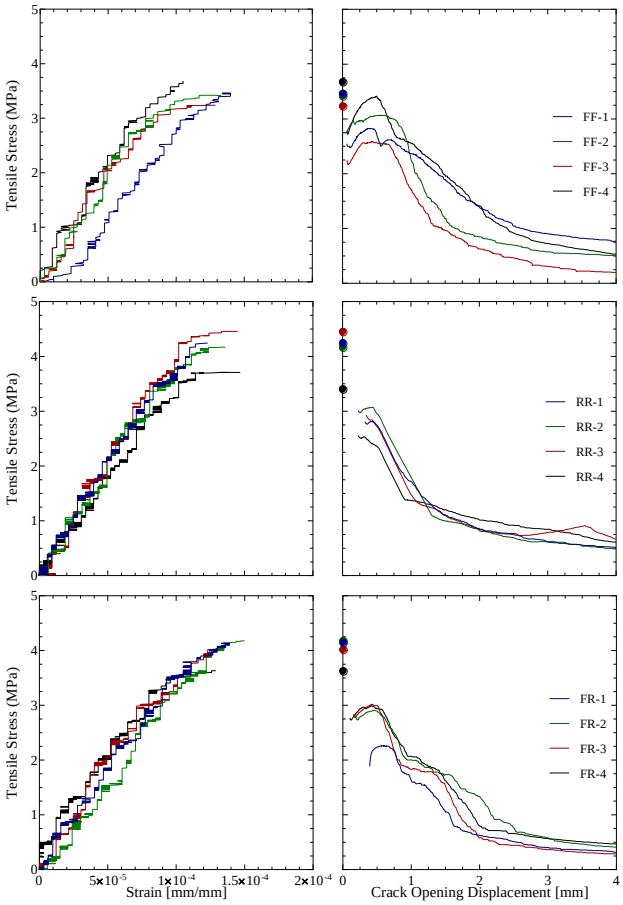

Figure 6: Results of UTT tests

The number of fibres crossing the failure plane was recorded after testing; these results are presented in Table 1. Amin et al. [16] derived an expression for the number of fibres,

N_f, crossing a fracture plane based on the expression derived by Aveston and Kelly [17] accounting for the crack navigating through the "weakest plane" :

$$N_f = 0.82\rho_f A_c/(2k_t A_f) \quad (1)$$

where ρ_f is the volumetric ratio of fibres, A_c is the cross sectional area of the failure crack, k_t is a fibre orientation correction factor taken as $k_t = 0.5 \le 1/(0.94 + 0.6 l_f/b) \le 1$, l_f is the fibre length, b is the width of a square fracture plane and A_f is the cross sectional area of an individual fibre. The predicted number of fibres crossing the crack using Equation 1 is 223, which correlates well with the observed numbers.

Table 1: Material Test Results

Dogbone ID	f_{ct} [MPa]	ε_t(x10^{-4}) [-]	E_t [GPa]	$f_{0.5}$ (MPa)	N_f [-]
FF-1	3.46	1.40	32.3	2.71	220
FF-2	3.42	1.33	35.3	3.06	241
FF-3	3.24	1.29	34.9	2.57	240
FF-4	3.68	1.17	35.3	3.42	273
Mean	3.45	1.30	34.5	2.94	244
COV	0.05	0.07	0.04	0.13	0.09
RR-1	4.25	1.23	37.6	2.75	257
RR-2	4.17	1.36	37.5	2.96	235
RR-3	4.46	1.45	43.2	2.73	233
RR-4	3.71	1.47	33.8	2.36	207
Mean	4.15	1.38	38.0	2.70	233
COV	0.08	0.08	0.10	0.09	0.09
FR-1	4.15	1.39	33.2	2.23	200
FR-2	4.18	1.50	35.0	2.90	261
FR-3	4.02	1.35	33.3	3.00	195
FR-4	3.63	1.29	32.9	2.94	219
Mean	4.00	1.38	33.6	2.77	219
COV	0.06	0.06	0.03	0.13	0.14

To investigate the progression of cracking within each specimen, it is important to consider the readings obtained from each transducer. The centre to centre distance between the North and South transducers was 175 mm, and the centre to centre distance between the East and West transducers was 265 mm. The measured in- and out-of-plane rotations at an average strain, $\varepsilon_t = 0.7\times10^{-4}$ [-] and COD of 0 mm (at peak load), 0.5 mm and 1.5 mm for each specimen are presented in Tables 2, 3, 4 and 5 respectively.

Table 2: Rotation of uniaxial tests at an average $\varepsilon_t = 0.7\times10^{-4}$

Dogbone ID	Out of plane rotation [mrad]	In plane rotation [mrad]
FF-1	0.137	-0.020
FF-2	0.017	0.041
FF-3	-0.034	-0.020
FF-4	-0.051	0.000
RR-1	-0.017	0
RR-2	0	-0.061
RR-3	0	-0.061
RR-4	0.017	-0.000
FR-1	0.017	-0.041
FR-2	0.051	-0.020
FR-3	0.017	-0.041
FR-4	0	-0.020

Table 3: Rotation of uniaxial tests at an average COD = 0 mm

Dogbone ID	Out of plane rotation [mrad]	In plane rotation [mrad]
FF-1	0	-0.142
FF-2	-0.137	0.325
FF-3	-0.360	0.102
FF-4	-0.257	0.000
RR-1	-0.086	0.061
RR-2	0	-0.223
RR-3	-0.086	-0.203
RR-4	-0.017	-0.365
FR-1	0.154	0
FR-2	0.206	0.000
FR-3	0.120	-0.223
FR-4	-0.326	0

Ideally no rotations should occur during testing. As expected, significant rotations were observed pre- and post-localisation of the dominant crack in specimens within series RR and FR. Note that, specimens in series FF experienced small, yet non-negligible end rotations. This indicates that, due to the flexibility of the end platens, and the specimen itself, the primary objective of fixing the boundaries, namely in the restraint of end

rotations, was only partially achieved in reality.

Table 4: Rotation of uniaxial tests at an average COD = 0.50 mm

Dogbone ID	Out of plane rotation [mrad]	In plane rotation [mrad]
FF-1	-9.223	-0.568
FF-2	-1.337	0.466
FF-3	-7.080	0.487
FF-4	-9.634	-1.175
RR-1	-8.863	1.987
RR-2	-10.234	-0.831
RR-3	-2.023	-7.887
RR-4	9.909	-0.426
FR-1	4.920	-4.501
FR-2	-8.040	1.176
FR-3	0.891	-5.514
FR-4	-7.971	2.048

Table 5: Rotation of uniaxial tests at an average COD = 1.50 mm

Dogbone ID	Out of plane rotation [mrad]	In plane rotation [mrad]
FF-1	-10.029	-0.162
FF-2	-2.983	4.298
FF-3	-8.691	3.954
FF-4	-16.646	-1.844
RR-1	-20.160	0.751
RR-2	-31.286	-0.506
RR-3	-0.737	-19.018
RR-4	20.126	-0.446
FR-1	5.640	-10.867
FR-2	-18.720	1.683
FR-3	1.971	-17.111
FR-4	-19.543	0.264

The distribution of fibres across the critical crack is presented in Figure 7 for each of these samples. Plotted too in Figure 7 is the centre of gravity of all fibres. Comparing the distribution of fibres in Figure 7, with the results listed in Tables 3-5, highlight that the in- and out-of-plane rotations of the dogbone specimens are proportional to the distribution of fibres through the thickness of the specimens, after the concrete has cracked. For regions where many fibres exist, the crack would be more restrained than in areas where fewer fibres are located. By way of example, examining the results for specimen FF-1 in Figure 7, the Northern face of the dogbone contained 27.7% of the total amount of fibres across the crack, whereas the Southern face contained 19.1% of fibres. At an average COD of 1.5 mm, the width of the cracks along the Northern and Southern faces were approximately 0.85 mm and 2.15 mm, respectively. Similar comparisons can be made with the results as shown in Tables 3-5. This implies that for softening SFRC, more force passes through the sample at the locations with more fibres, and at these locations the cracks are expected to be narrower. Hence there is a non-uniform distribution of stress along the fracture plane of the sample. In these instances, for the RR series, as the universal joints are allowed to freely rotate, the specimens are unrestrained and will undergo significant bending, as observed until the resultant tensile force carried by the fibres matches the imposed tensile force and line of action provided by the UTM.

5 CONCLUSIONS

This paper presents the results of an experimental campaign aiming to identify the influence of the boundary effects on the recently released Australian uniaxial tension test for SFRC. Three boundary conditions are possible: fixed-fixed, fixed-rotating, and rotating-rotating. The main conclusions stemming from this study are as follows:

- The fixed-fixed condition results in cracking stresses lower than the ones obtained with fixed-rotating and rotating-rotating conditions;
- Due to the flexibility of the end platens and the specimen itself, non-negligible rotations occur with the fixed-fixed end conditions;
- Specimens with rotating-rotating end conditions displayed significant out of plane rotation during testing as a result of the heterogeneous distribution of fibres through the thickness of the member;

• The fixed-rotating end condition serves as a compromise to the issues associated with the other test setups and seems to be more suited for uniaxial tension testing of SFRC.

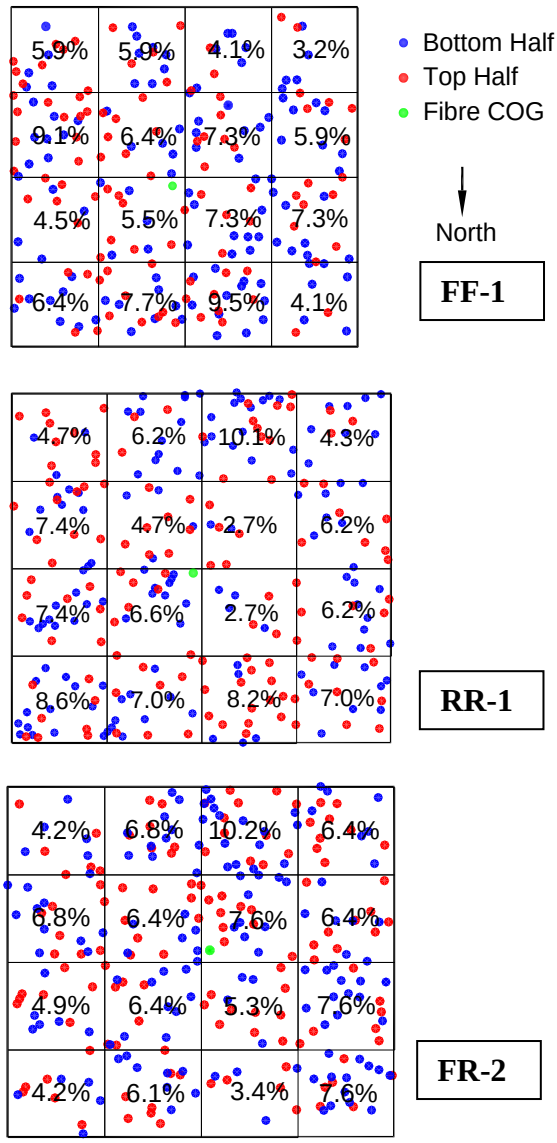

Figure 7: Fibre distribution of cracked section

REFERENCES

[1] Van Mier, J.G.M., 1997. *Fracture Processes of Concrete*. CRC Press.

[2] Kooiman, A.G., 2000. Modelling steel fibre reinforced concrete for structural design. *PhD Dissertation*, Delft University of Technology, The Netherlands.

[3] Löfgren, I., 2005. Fibre reinforced concrete for industrial construction – a fracture mechanics approach to material testing and structural analysis. *PhD Dissertation*, Chalmers University of Technology, Sweden.

[4] Rots, J.G. and de Borst, R., 1998. Analysis of concrete fracture in 'direct' tension. *Int. J. Solids. Struc*. **25(12)**:1381-94.

[5] Cattaneo, S., Rosati, G., and Banthia, N., 2009. A simple model to explain the effect of different boundary conditions in direct tension tests. *Cons. Build. Mater*. **23**:169-84.

[6] Bažant, Z. P., and Planas, J., 1998. *Fracture and size effect in concrete and other quasibrittle materials*. CRC Press.

[7] AS5100.5. 2017. Bridge Design Part 5: Concrete. Australian Standard, *Standards Association of Australia*.

[8] AS3600. 2018. Concrete Structures. Australian Standard, *Standards Association of Australia*.

[9] van Vliet, M.R.A., 2000. Size effect in tensile fracture of concrete and rock. *PhD Dissertation*, Delft University of Technology, The Netherlands.

[10] Susetyo, J., 2009. Fibre reinforcement for shrinkage crack control in prestressed, precast segmental bridges. *PhD Dissertation*, The University of Toronto, Canada.

[11] Luo, J. W., 2014. Behaviour and analysis of steel fibre-reinforced concrete under reversed cyclic loading. *MASc Dissertation*, The University of Toronto, Canada.

[12] Isojeh, B., 2017. Fatigue damage analysis of reinforced concrete structural elements. *PhD Dissertation*, The University of

Toronto, Canada.

[13] EN14651. 2007. Test method for metallic fibre concrete- measuring the flexural tensile strength (LOP, residual). *European committee for standardization*.

[14] Amin, A., 2015. Post cracking behaviour of steel fibre reinforced concrete: from material to structure. *PhD Dissertation*, The University of New South Wales, Australia.

[15] Amin, A., Markic, T., Gilbert, R. I., and Kaufmann, W., 2018. Effect of the boundary conditions on the Australian uniaxial tension test for softening steel fibre reinforced concrete. *Cons. Build. Mater*. **184**:215-28.

[16] Amin, A., Foster, S. J., and Kaufmann, W., 2017. Instantaneous deflection calculation for steel fibre reinforced concrete one way members. *Eng. Struc.* **131**:438-45.

[17] Aveston, J., and Kelly, A., 1973. Theory of multiple fracture of fibrous composites. *J. Mater. Sci.* **8(3)**:352-62.

ACKNOWLEDGMENTS

The experimental work conducted in this paper was undertaken using the facilities at the Heavy Structures Laboratory at the University of New South Wales, Australia. We acknowledge this support with thanks.